Engineering Structures 78 (2014) 90–99

Contents lists available at ScienceDirect

Engineering Structures

journal homepage: www.elsevier.com/locate/engstruct

Performance-based seismic risk assessment for buildings equipped with linear and nonlinear viscous dampers

E. Tubaldi [a], M. Barbato [b,*], A. Dall'Asta [a]

[a] School of Architecture and Design, University of Camerino, Viale della Rimembranza, 63100 Ascoli Piceno (AP), Italy
[b] Department of Civil & Environmental Engineering, Louisiana State University and A&M College, 3418H Patrick F. Taylor Hall, Nicholson Extension, Baton Rouge, LA 70803, USA

ARTICLE INFO

Article history:
Available online 12 June 2014

Keywords:
Performance-based earthquake engineering
Seismic risk assessment
Viscous dampers
Non-stationary random process

ABSTRACT

This paper introduces an efficient methodology for assessing the seismic risk of structural systems equipped with linear and nonlinear viscous damping devices while accounting for the uncertainties affecting both seismic input and model parameters. The proposed methodology employs a combination of efficient and accurate analytical and simulation techniques to estimate the probabilistic properties of the structural response under a seismic input modeled as a non-stationary stochastic process.

The effectiveness of the proposed methodology is illustrated through a parametric study, with respect to the dampers' properties, of the performance of two adjacent steel buildings connected by linear and nonlinear viscous dampers. The results of the study provide useful information regarding the accuracy of the approximations introduced by the proposed reliability assessment approach, and the effectiveness of the added dampers in reducing the system seismic risk.

1. Introduction

In the last two decades, the use of viscous and visco-elastic dampers has become increasingly widespread in the design and retrofit of civil structures excited by wind and earthquake loads, due to the capability of these devices to mitigate undesirable aspects of the structural response [1,2]. Experimental and analytical studies have demonstrated that viscous dampers placed inside the buildings or between adjacent buildings permit to control and significantly mitigate the motion amplitude, interstory drifts, and absolute accelerations induced by earthquake actions [2–9].

The assessment of the seismic reliability of structures equipped with viscous/visco-elastic damping devices is a complex task that requires a probabilistic approach in order to rigorously account for the uncertainties that characterize the seismic input (record-to-record and intensity variability), as well as the properties of the structural systems and of their models (model parameter uncertainty (MPU)) [10–15]. Although stochastic simulation procedures (e.g., direct Monte Carlo simulation (MCS) [12,13] or subset simulation [16,17]) can be employed to solve this type of problem, they usually require a very large number of analyses to obtain accurate results when small failure probabilities need to be estimated. Thus, when possible, analytical techniques based on random vibration theory are preferred to direct stochastic simulation techniques [18–23]. In fact, several methodologies available in the literature employed analytical techniques for the probabilistic assessment and reliability-based design of viscously damped systems [3–6,9]. However, the complexity of the analytical treatment of this problem led to the adoption of numerous simplifications concerning the reliability evaluation, the seismic input description, and the uncertainty of the structural models. With regard to the reliability evaluation, many existing procedures focused only on the mean-square response of the buildings, without explicit reliability considerations regarding the structural performance as measured by the risk of damage and losses (see [9] for a comparison of different stochastic performance measures for stationary response). Furthermore, only few studies considered the effects on the system reliability of the statistical dependence among different failure modes, albeit these effects can be very significant [9]. With regard to the seismic input description, numerous studies employed oversimplified stochastic models that neglect the non-stationarity of earthquake ground motion. Finally, regarding the uncertainty of the structural models, a significant portion of the research performed in this field disregarded the effects of MPU, which can have a non-negligible influence on the structural performance [10–15].

This study presents a hybrid approach that combines efficient analytical and simulation techniques for reliability analysis to

* Corresponding author.
E-mail addresses: etubaldi@gmail.com (E. Tubaldi), mbarbato@lsu.edu (M. Barbato), a.asta@tin.it (A. Dall'Asta).

http://dx.doi.org/10.1016/j.engstruct.2014.04.052
0141-0296/

estimate the seismic risk of structural systems equipped with linear or nonlinear viscous dampers. This approach accounts for the correlation between different failure modes, the non-stationarity of the earthquake ground motion excitation, and the effects on system reliability of MPU. In the first part of the paper, the direct reliability problem consisting in the evaluation of the seismic risk is formulated consistently with modern performance-based earthquake engineering (PBEE) frameworks, such as the Pacific Earthquake Engineering Research Center (PEER) PBEE framework [24,25]. Successively, the problem solution is presented for the case of structural systems and performance levels for which the hypothesis of linear structural behavior is satisfied with good accuracy. The effects of the seismic input uncertainty are taken into account through random vibration techniques. In particular, in the case of linear dampers, recently derived closed-form analytical solutions [21] for the statistics of the stochastic structural response are employed. In the case of nonlinear dampers, an existing stochastic linearization technique is used to efficiently estimate the response statistics [26,27]. In both the cases, a simulation approach based on Latin hypercube sampling [28] is proposed to account for the uncertainty in the model parameters.

The proposed methodology is applied in this paper to evaluate the seismic risk of two adjacent steel buildings coupled by viscous dampers. A parametric study is performed to investigate the influence of the damper properties and nonlinearity level on the risk estimates. Comparisons with pertinent MCS results are made to assess the accuracy of the proposed approach.

2. Formulation of the reliability-based assessment problem

2.1. Mean annual frequency of limit state exceedance based on the PEER PBEE framework

The PEER PBEE framework [24,25] is a general probabilistic methodology for the performance assessment of structures subjected to seismic hazard. The aim of the framework is to evaluate the mean annual frequency (MAF) of exceedance of a decision variable (i.e., of a measurable attribute of a specific structural performance that can be defined in terms of cost/benefit for the users and/or the society). The computation of the decision variable is disaggregated into the following four probabilistic analysis components: (1) probabilistic seismic hazard analysis, which describes the uncertainty of the ground-motion intensity measures (IMs); (2) probabilistic seismic demand analysis, which describes the uncertainty of the engineering demand parameters (EDPs) used to monitor the structural response conditional on the IMs; (3) probabilistic seismic damage analysis, which describes the uncertainty of the damage measures (DMs) or limit states that can be correlated with the chosen decision variable; and (4) probabilistic seismic loss analysis, which describes the uncertainty of the decision variable. The reliability-based procedure developed in this paper involves only the first three steps of the framework since it provides the MAF of exceedance of a set of specified limit states related to the building components (e.g., structural elements and dampers). This MAF can be expressed as:

$$\nu_{\mathbf{DM}}(\mathbf{dm}) = \int_{\mathbf{im}} \int_{\mathbf{edp}} G_{\mathbf{DM}|\mathbf{EDP}}(\mathbf{dm}|\mathbf{edp}) \cdot |\mathrm{d}G_{\mathbf{EDP}|\mathbf{IM}}(\mathbf{edp}|\mathbf{im})| \cdot |\mathrm{d}\,\nu_{\mathbf{IM}}(\mathbf{im})| \quad (1)$$

in which $\nu_{\mathbf{IM}}(\mathbf{im})$ denotes the MAF of exceeding a given value **im** of the vector of IMs; $G_{\mathbf{EDP}|\mathbf{IM}}(\mathbf{edp}|\mathbf{im})$ denotes the complementary (joint) cumulative distribution function of the vector of EDPs, **EDP**, conditional on **IM = im**; and $G_{\mathbf{DM}|\mathbf{EDP}}(\mathbf{dm}|\mathbf{edp})$ denotes the complementary (joint) cumulative distribution function of the vector of DMs, **DM**, conditional on **EDP = edp**. In this paper, for the IMs, EDPs, and DMs, upper case letters denote random quantities, lower case letters denote specific realizations, italic characters denote scalar quantities, and bold characters denote vector quantities.

An important intermediate result of the PBEE procedure is given by the following convolution integral:

$$P_{\mathbf{DM}|\mathbf{IM}}(\mathbf{im}) = \int_{\mathbf{edp}} G_{\mathbf{DM}|\mathbf{EDP}}(\mathbf{dm}|\mathbf{edp}) \cdot |\mathrm{d}G_{\mathbf{EDP}|\mathbf{IM}}(\mathbf{edp}|\mathbf{im})| \quad (2)$$

which provides the probability of exceedance of the considered damage limit states conditional on the seismic intensity. For each damage limit state, Eq. (2) can be specialized as:

$$P_{DM_i|\mathbf{IM}}(\mathbf{im}) = \int_{\mathbf{edp}} G_{DM_i|\mathbf{EDP}}(dm_i|\mathbf{edp}) \cdot |\mathrm{d}G_{\mathbf{EDP}|\mathbf{IM}}(\mathbf{edp}|\mathbf{im})| \; ; \quad i = 1, 2, \ldots, N_{ls} \quad (3)$$

in which DM_i and dm_i denote the i-th components of vector **DM** and **dm**, respectively, N_{ls} denotes the number of limit states, and $P_{DM_i|\mathbf{IM}}(\mathbf{im})$ denotes the probability of exceedance of the i-th damage measure (limit state) conditional on **IM = im**. Combining Eqs. (1) and (2) gives the MAFs of exceedance of damage level **DM = dm**:

$$\nu_{\mathbf{DM}}(\mathbf{dm}) = \int_{\mathbf{im}} P_{\mathbf{DM}|\mathbf{IM}}(\mathbf{im}) \cdot |\mathrm{d}\,\nu_{\mathbf{IM}}(\mathbf{im})| \quad (4)$$

2.2. Seismic risk assessment as a direct reliability problem

Seismic risk assessment consists in computing the probability that a structure exceeds any specified damage level or limit state (at a component and/or system level) during its assumed design life, t_L. In this type of direct reliability problems, the structural properties of the building and the mechanical properties of the dampers, as well as the seismic input characteristics at the building site, are uncertain quantities for which a probabilistic description is available. This paper considers discrete limit states only, using a similar approach as that followed in numerous PBEE studies available in the literature [25].

The evaluation of the reliability of a multi-component structural system requires selecting suitable limit states that are correlated with the components' performance. This study focuses on limit states related to structural damage, and the interstory drifts (defined as the difference in the lateral deflection measured at the top and bottom of a story, and divided by the story height) are employed as global EDPs [29,30]. Several guidelines and seismic codes provisions [31,32] provide the values of the interstory drifts corresponding to different limit states and/or structural performance levels. It is noteworthy that other EDPs (e.g. absolute floor accelerations) and limit states can be of interest in monitoring the performance of buildings [9,33,34]. The performance of the dampers is another important aspect in evaluating the system reliability, since the proper and continuous operation of the damping devices is critical in ensuring that the buildings achieve the desired target performance level. In the literature, limits are considered for the shear deformation that can be attained in visco-elastic dampers [4,35], or for both the stroke (displacement) and force demand in fluid viscous dampers [36]. The computation of the conditional probability of failure of the components $P_{DM_i|\mathbf{IM}}(\mathbf{im})$ and of the system $P_{f|\mathbf{IM}}(\mathbf{im})$ requires solving a time-variant reliability problem by accounting for the pertinent sources of uncertainty, e.g., randomness in the seismic input and MPU. The probability $P_{f|\mathbf{IM}}(\mathbf{im})$ is a special case of the probability $P_{\mathbf{DM}|\mathbf{IM}}(\mathbf{im})$ given in Eq. (2), which is obtained when discrete limit states are considered. The plot of $P_{f|\mathbf{IM}}(\mathbf{im})$ versus **IM** is commonly called fragility curve in the literature [25].

The system failure probability conditional on **IM = im**, $P_{f|\mathbf{IM}}(\mathbf{im})$, depends on the system configuration and on the statistical

dependence among the component limit states [37,38]. Regarding the system configuration, this study considers a series idealization (i.e., the system failure is attained when any of the N_{ls} component limit states is exceeded), which is commonly used in the literature for the type of problem under study [4–6]. With regard to the statistical dependence among the component limit states, stochastic simulation techniques can accurately account for it when estimating $P_{f|\mathbf{IM}}(\mathbf{im})$ [13]. Conversely, the analytical evaluation of the system failure probability is usually extremely complex, and different approximate solutions are commonly used [4–6,9]. In this study, analytical solutions in conjunction with reliability bounds are adopted and compared with MCS results.

Once $P_{f|\mathbf{IM}}(\mathbf{im})$ is known, the MAF of system failure, ν_f, can be computed by convolution with the seismic hazard curve as in Eq. (4), i.e.,

$$\nu_f = \int_{\mathbf{im}} P_{f|\mathbf{IM}}(\mathbf{im}) \cdot |\mathrm{d}\nu_{\mathbf{IM}}(\mathbf{im})| \tag{5}$$

Furthermore, assuming that the occurrence of the event of system failure can be described by a Poisson process, the value of the system failure probability during the design life time, P_{f,t_L}, can be evaluated as

$$P_{f,t_L} = 1 - e^{-\nu_f \cdot t_L} \tag{6}$$

3. Efficient technique for seismic assessment of linear elastic systems with dampers

This section illustrates an efficient combination of analytical and simulation techniques that can be used to solve the direct reliability problem defined by Eqs. (5) and (6). First, the system equations of motion and the seismic input model are described. Then, the analytical techniques for computing the conditional failure probability $P_{f|\mathbf{IM}}(\mathbf{im})$ in the case of deterministic system and for both linear and nonlinear dampers are illustrated. Finally, a simulation technique for including the effects of MPU is proposed.

3.1. Equations of motion for linear systems with added dampers

The equations of motion of linear systems with added dampers can be written as follows:

$$\mathbf{M} \cdot \ddot{\mathbf{u}}(t) + \mathbf{C} \cdot \dot{\mathbf{u}}(t) + \mathbf{K} \cdot \mathbf{u}(t) + \mathbf{f}_d(t) = -\mathbf{M} \cdot \mathbf{R} \cdot \ddot{\mathbf{u}}_g(t) \tag{7}$$

in which $\mathbf{u}$ denotes the displacement vector of the free degrees-of-freedom (DOFs); $\mathbf{M}$, $\mathbf{K}$, and $\mathbf{C}$ denote the mass, stiffness, and damping matrices, respectively; $\mathbf{f}_d(t)$ denotes the vector of the resisting forces produced by the added dampers; $\mathbf{R}$ denotes the load distribution matrix; $\ddot{\mathbf{u}}_g(t)$ denotes the vector containing the different components of the input ground motion; t denotes time; and a superposed dot denotes differentiation with respect to time.

The resisting force corresponding to the j-th damper (i.e., the j-th component of $\mathbf{f}_d(t)$) depends on the relative displacement and/or velocity at the two ends of the damper and can be expressed as:

$$f_{dj}(t) = k_{dj} \cdot \Delta u_j(t) + c_{dj} \cdot |\Delta \dot{u}_j(t)|^{\alpha_j} \cdot \mathrm{sign}[\Delta \dot{u}_j(t)]; \quad j = 1, 2, \ldots, N_d \tag{8}$$

where N_d denotes the number of dampers; α_j denotes the j-th damper exponent (equal to one in case of linear dampers); $\Delta u_j(t)$ denotes the relative displacement between the j-th damper's ends (which is linearly related to vector $\mathbf{u}$); k_{dj} and c_{dj} denote the j-th damper's stiffness and viscous constant, respectively; and sign$(\cdot)$ denotes the sign function.

In this paper, the input ground acceleration components are modeled as separable non-stationary stochastic processes [21]. This analytical representation of the seismic input is defined by a power spectral density (PSD) function of an embedded Gaussian stationary process and by a deterministic time-modulating function. The description of the seismic input is completed by an appropriate seismic hazard function for the site, the definition of which entails selecting the seismic IMs and computing the corresponding MAF of exceedance $\nu_{\mathbf{IM}}(\mathbf{im})$. The IMs selection should be driven by sufficiency and efficiency criteria [39]. In addition, the IMs must be easily related to the stochastic description of the input ground motion process. While the proposed methodology is independent of the IMs' choice, a scalar intensity measure, *IM*, is considered hereinafter for the sake of clarity and simplicity.

3.2. Seismic risk assessment for deterministic model properties

The i-th component fragility function $P_{\mathbf{DM}_i|IM}(im)$ given by Eq. (2) is obtained in this paper as the solution of a first-passage reliability problem for a scalar process, which can be expressed as follows [40]

$$P_{DM_i|IM}(im) = 1 - P\left[g_{i|IM}(t=0|im) > 0\right] \cdot \exp\left\{-\int_0^{t_{\max}} h_{i|IM}(\tau|im) \cdot \mathrm{d}\tau\right\}; \quad i = 1, 2, \ldots, N_{ls} \tag{9}$$

in which $h_{i|IM}(t|im)$ denotes the time-variant hazard function relative to the i-th limit state conditional on $IM = im$ (i.e., the failure rate at time t conditioned on having no failure before time t and on $IM = im$), $g_{i|IM}(t|im) = \zeta_i - EDP_{i|IM}(t|im)$ denotes the i-th time-variant limit state function conditional on $IM = im$, and ζ_i denotes the i-th component limit state threshold. For structural systems with at rest initial conditions, the probability of survival at time $t = 0$ is $P[g_{i|IM}(t = 0|im) > 0] = 1$.

Several analytical approximations are available in the literature for $h_{i|IM}(t|im)$, e.g., the Poisson's (P), the classical Vanmarcke's (cVM), and the modified Vanmarcke's (mVM) approximations [22,40]. The use of the P approximation of the time-variant hazard function involves computing the time history of the variances of the **EDP** components and of their first time-derivatives, as well as the correlation coefficient between the **EDP** components and their corresponding first time-derivatives [21]. In addition to these quantities, the use of the cVM and mVM approximations requires computing the time-variant first-order non-geometric spectral characteristics that are needed to evaluate the bandwidth parameters of the components of **EDP** [21]. It is noteworthy that the additional computational cost of the cVM and mVM is justified by the fact that these approximations are, in general, significantly more accurate than the P approximation [14,22,23].

In this paper, the structural response statistics needed to analytically estimate the hazard function $h_{i|IM}(t|im)$ are obtained using the closed-form solutions developed in [21] for the case of linear dampers, and the stochastic linearization technique described in [27] for the case of nonlinear dampers. The analytical formulation presented in [21] is based on state-space complex modal analysis, which is suitable for both classically and non-classically damped MDOF systems subjected to the earthquake model described above, and on complex plane integration to compute the spectral characteristics of the complex-valued modal response processes. The stochastic linearization technique introduced in [27] involves evaluating, at each time instant, the properties of equivalent linear dampers, which minimize the mean square difference between the nonlinear damper force and the equivalent linear damper force. These equivalent properties depend on the system stochastic response through the formula:

$$c_{d,eqj}(t) = c_{dj} \cdot \frac{2^{1+\frac{\alpha_j}{2}} \cdot \Gamma\left(1+\frac{\alpha_j}{2}\right)}{\sqrt{2\pi}} \cdot \sigma_{\Delta \dot{u}_j}^{\alpha_j - 1}(t); \quad j = 1, 2, \ldots, N_d \tag{10}$$

where $c_{d,eqj}(t)$ is the equivalent viscous constant of the damper, $\sigma_{\Delta\dot{u}_j}(t)$ is the standard deviation of the relative velocity between the j-th damper's ends, and $\Gamma(\cdot)$ denotes the Gamma function.

The equivalent viscous constant of the dampers are evaluated via an iterative procedure [27], which also provides the evolution of the response covariance matrix. Based on this matrix, the conditional probability of failure is evaluated here by assuming a P approximation of the time-variant hazard function.

In this study, in order to balance the requirements of computational efficiency and accuracy of the proposed assessment procedure, upper and lower bounds of the conditional system failure probability $P_{f|IM}(im)$ are considered in conjunction with the analytical estimates of the conditional component failure probabilities $P_{DM_i|IM}(im)$. These bounds are obtained by introducing the assumptions of independent and perfectly correlated component failures as [37]:

$$P^{ub}_{f|IM}(im) = 1 - \prod_{i=1}^{N_{ls}} \left[1 - P_{DM_i|IM}(im)\right]$$
$$P^{lb}_{f|IM}(im) = \max_{1\le i\le N_{ls}} \left[P_{DM_i|IM}(im)\right] \quad (11)$$

respectively.

3.3. Effects of model parameter uncertainty

In this study, the uncertainty affecting the parameters used to define both the structural model (e.g., building geometry, stiffness, damping, inertia, and damper properties) and the limit states (e.g., uncertain drift capacity and damper capacity) is referred to as MPU. Similar to [14], the effects of this uncertainty are accounted for by using the total probability theorem and the Latin hypercube sampling technique [28]. The conditional probability of failure is expressed as:

$$P_{f|IM}(im) = \int_{\mathbf{X}} P_{f|IM,\mathbf{X}}(im,\mathbf{x}) \cdot f(\mathbf{x}) \cdot \mathrm{d}\mathbf{x} \quad (12)$$

in which $\mathbf{X}$ denotes the vector of uncertain model parameters with joint probability density function $f_{\mathbf{X}}(\mathbf{x})$, and $P_{f|IM,\mathbf{X}}(im,\mathbf{x})$ denotes the probability of failure conditional on $\mathbf{X}$ and $IM = im$.

Using the Latin hypercube sampling technique, samples of vector $\mathbf{X}$ are generated and employed to define a set of deterministic models with deterministic limit states. For each of these sample models and limit states, the conditional system failure probability $P_{f|IM,\mathbf{X}}(im,\mathbf{x})$ can be computed via stochastic simulation or by using an analytical approximation based on Eqs. (9) and (11). It is noteworthy that MPU is non-ergodic in nature [24]. Thus, Eq. (5) still holds when $P_{f|IM}(im)$ is computed using Eq. (12) in order to account for MPU effects. However, as demonstrated in [24], the MAF of failure obtained from Eqs. (12) and (5) cannot be directly employed to evaluate the system risk via Eq. (6), because this procedure would violate the Poisson's assumption on which Eq. (6) is based. This study employs the following formula, for which the Poisson's assumption is still valid:

$$P_{f,t_L} = 1 - \int_{\mathbf{X}} e^{-\nu_f(\mathbf{x})\cdot t_L} \cdot f(\mathbf{x}) \cdot \mathrm{d}\mathbf{x} \quad (13)$$

The Latin hypercube sampling approach used in this study has some advantages over other existing approaches that are commonly employed to incorporate the effects of MPU, such as MCS or the perturbation method [11]. In fact, Latin hypercube sampling is more efficient in spanning the sample space and, thus, requires fewer samples than MCS to achieve the same level of accuracy. Furthermore, the accuracy of Latin hypercube sampling is not affected by the values of the coefficients of variation of the uncertain model parameters, in contrast with first- and second-order perturbation approaches [41].

4. Application examples

In this section, the proposed methodology is applied to the seismic risk assessment of two adjacent buildings coupled by using linear and nonlinear viscous dampers. Three different cases are considered: (1) buildings with deterministic properties coupled by linear viscous/visco-elastic dampers, (2) buildings with uncertain properties coupled by linear viscous dampers, and (3) buildings with deterministic properties coupled by nonlinear viscous dampers. The case of buildings with uncertain properties coupled by nonlinear viscous dampers is not presented here, due to space constraints and because it does not provide additional insight into the problem at hand when compared to the other cases considered in this paper. For each of the three cases considered here, a parametric study is performed to investigate the effects on the seismic risk of the damper properties (i.e., viscous constant for all cases, stiffness constant for the case of deterministic buildings with linear dampers, and damper exponent for the case of buildings coupled by nonlinear dampers). The same seismic input is considered throughout all the examples.

These application examples focus on the probability of exceeding the Immediate Occupancy (IO) performance level in any of the two buildings during their design life time of 50 years. For this purpose, a series idealization is considered for the system, by assuming that its failure corresponds to the exceedance of an inter-story drift ratio (IDR) limit of 0.7% by any of the two buildings' stories. This IDR value can be considered as a conventional limit for the linear elastic behavior of multi-story steel buildings and for their IO limit state, which corresponds to negligible structural damage [31,32]. Thus, the assumption of linear elastic behavior is deemed accurate for this specific application, since the fact that the buildings may experience nonlinear behavior for high (and rare) IM values does not introduce bias into the risk estimates for the IO limit state.

4.1. Case study and seismic input description

The adjacent buildings considered in this study are two steel moment-resisting frames with shear-type behavior (Fig. 1), whose mechanical and geometric properties are taken from [14]. Building A is an eight-story frame with constant floor mass, m_A = 454,540 kg, and stiffness, k_A = 628,801 kN/m. Building B is a four-story building with constant story mass, m_B = 454,540 kg, and stiffness, k_B = 470,840 kN/m. The story heights are equal to 3.2 m.

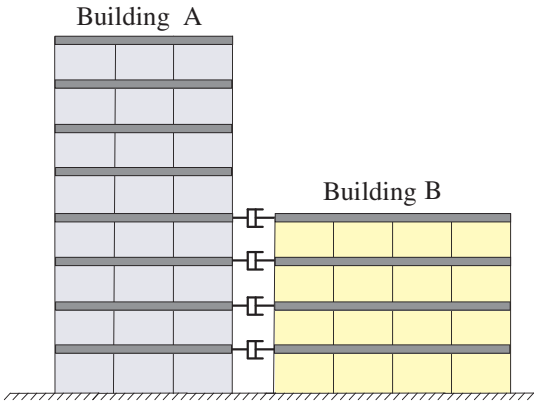

Fig. 1. Schematic representation of adjacent buildings coupled by damping devices.

The motion of the coupled system is described by Eq. (7), in which the mass, stiffness, and damping matrix are expressed as $\mathbf{M} = \begin{bmatrix} \mathbf{M}_A & \mathbf{0} \\ \mathbf{0} & \mathbf{M}_B \end{bmatrix}$, $\mathbf{K} = \begin{bmatrix} \mathbf{K}_A & \mathbf{0} \\ \mathbf{0} & \mathbf{K}_B \end{bmatrix}$, and $\mathbf{C} = \begin{bmatrix} \mathbf{C}_A & \mathbf{0} \\ \mathbf{0} & \mathbf{C}_B \end{bmatrix}$, respectively, where $\mathbf{M}_i$, $\mathbf{K}_i$, and $\mathbf{C}_i$ denote the mass, stiffness, and damping matrices of building i (i = A, B). Matrices $\mathbf{C}_A$ (with dimensions 8 × 8) and $\mathbf{C}_B$ (with dimensions 4 x 4) describe the inherent buildings' damping and are based on the Rayleigh model by assuming a damping factor $\xi_A = \xi_B = 2\%$ for the first two vibration modes of each system. The fundamental vibration periods of building A and B are $T_A = 0.915$ s and $T_B = 0.562$ s, respectively.

Similar to [14,42], the stochastic seismic input used in the application examples is modeled as a Gaussian stationary process modulated in time through the Shinozuka-Sato's function [43]

$$I(t) = c \cdot (e^{-b_1 \cdot t} - e^{-b_2 \cdot t}) \cdot H(t) \tag{14}$$

in which $b_1 = 0.045\pi s^{-1}$, $b_2 = 0.050\pi s^{-1}$, $c = 25.812$, and $H(t)$ is the unit step function. A duration $t_{max} = 30$ s is considered for the seismic excitation. The PSD function of the stationary process is described by the widely-used Kanai–Tajimi model, as modified by Clough and Penzien [44], i.e.,

$$S_{CP}(\omega) = S_0 \cdot \frac{\omega_g^4 + 4 \cdot \xi_g^2 \cdot \omega^2 \cdot \omega_g^2}{\left[\omega_g^2 - \omega^2\right]^2 + 4 \cdot \xi_g^2 \cdot \omega^2 \cdot \omega_g^2} \cdot \frac{\omega^4}{\left[\omega_f^2 - \omega^2\right]^2 + 4 \cdot \xi_f^2 \cdot \omega^2 \cdot \omega_f^2} \tag{15}$$

in which S_0 denotes the amplitude of the bedrock excitation, modeled as a white noise process; ω_g and ξ_g denote the circular frequency and damping factor of the soil, respectively; and ω_f and ξ_f denote the parameters describing the Clough–Penzien filter. The following values of the parameters are used hereinafter: $\omega_g = 12.5$ rad/s, $\zeta_g = 0.6$, $\omega_f = 2$ rad/s, and $\zeta_f = 0.7$. Fig. 2a shows the PSD function corresponding to Eq. (15) for $S_0 = 1$ m^2/s^3.

The peak ground acceleration (PGA) is assumed here as IM. In order to derive the fragility curves in terms of the selected IM, the relationship between the parameter S_0 of the modified Kanai–Tajimi spectrum and the PGA at the site is assessed based on the procedure reported in [14]. The site seismic hazard curve (Fig. 2b) is:

$$\nu_{PGA}(pga) = 6.734 \cdot 10^{-5} \cdot pga^{-2.857} \tag{16}$$

Thus, for the site of interest, a PGA value of 0.3 g (where g is the gravity constant) corresponds to $S_0 = 0.013$ m^2/s^3 and to a probability of being exceeded equal to 10% in 50 years (i.e., it has a return period of 475 years).

4.2. Seismic risk assessment for buildings with deterministic properties and coupled by linear dampers

This section presents the case of deterministic buildings coupled by linear dampers. These dampers connect the two buildings at the first four floors and have the same properties at all floors.

Fig. 3 illustrates the stochastic response of the coupled adjacent buildings for different values of c_d, $k_d = 0$ kN/m, and $pga = 0.3$ g. The value $c_d = 0$ kN s/m corresponds to uncoupled buildings. The value $c_d = 6000$ kN s/m corresponds to a very high dissipating capacity of the connecting viscous dampers and a damping ratio for the first vibration mode of the coupled system close to one. For $k_d = 0$ kN/m, the value $c_d = 1363.5$ kN s/m (resulting in a damping factor for the first vibration mode of about 0.16) corresponds to a 10% failure probability over 50 years for the coupled buildings.

Fig. 3a plots the time history of the standard deviation of the IDR at the first story of building A and B (denoted respectively as $\sigma_{IDR,A1}$ and $\sigma_{IDR,B1}$). The values of the IDR standard deviations are highest at the first stories of the buildings, due to the shear-type behavior and the uniform column stiffness along the building heights. Thus, the failure of these stories is expected to provide the largest contribution to the system failure probability. From Fig. 3a, it is observed that coupling the buildings with dampers significantly reduces both $\sigma_{IDR,A1}$ and $\sigma_{IDR,B1}$. However, an increase of the viscous constant c_d does not necessarily correspond to a decrease of the standard deviation of the IDR response for both buildings. In fact, the maximum values of $\sigma_{IDR,A1}$ and $\sigma_{IDR,B1}$ over the seismic input duration are equal to 0.29% and 0.21%, respectively, for $c_d = 1363.5$ kN s/m, whereas they are 0.24% and 0.26%, respectively, for $c_d = 6000$ kN s/m.

Fig. 3b plots the time histories of the correlation coefficient between the interstory drift of the first and eighth (top) story of building A, $\rho_{A1,A8}$, and the correlation coefficient between the interstory drifts of the first story of each building, $\rho_{A1,B1}$. The interstory drift of the first story of building A is highly correlated with the interstory drift of the top story of the same building for any value of c_d. Conversely, the correlation coefficient between the interstory drifts of the first stories of the two buildings depends significantly on the values of c_d. In fact, after a few seconds of excitation during which the correlation coefficient is very high for any value of c_d, the interstory drifts become almost statistically uncorrelated for $c_d = 0$ kN s/m and their correlation coefficients reach a practically constant value that increases for increasing c_d. This phenomenon derives from the different dynamic properties of buildings A and B. For short periods of time after the beginning of the excitation, the transient response of the two structures is dominated by the properties of the excitation. After the first part of the transient response, the two buildings tend to respond differently to the excitation. However, if the dampers connecting the two buildings have a high c_d value, the two buildings are forced to respond as a single system.

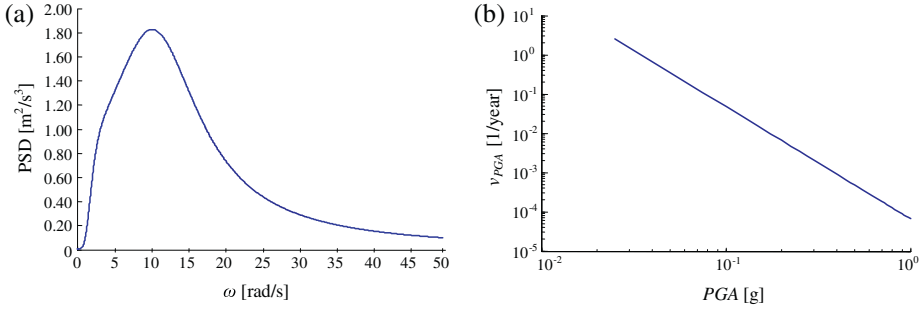

Fig. 2. Input ground motion: (a) PSD function of the stationary process for positive circular frequencies, and (b) site hazard curve.

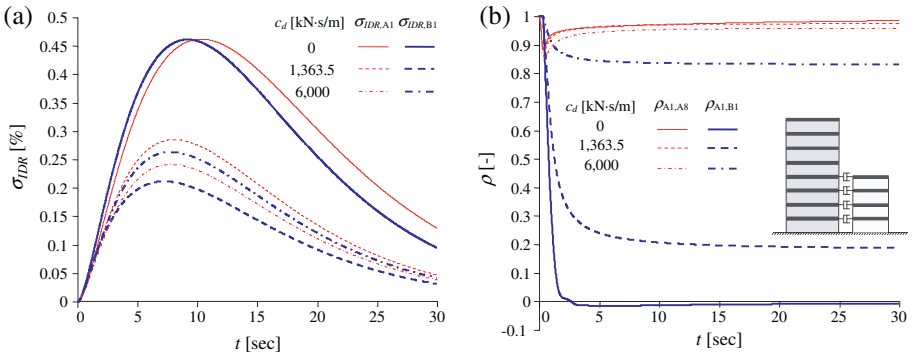

Fig. 3. Stochastic response of adjacent buildings coupled using purely viscous dampers with different c_d values: (a) time history of the standard deviation of the interstory drift responses, and (b) time history of the correlation coefficients of the interstory drift responses.

The seismic fragility and risk for the coupled buildings are obtained here by employing the analytical estimates of the time-variant hazard function presented in [22]. The accuracy of these analytical estimates is verified by comparing the results with those obtained through MCS, assumed as reference solution. The MCS results are based on time history analyses of linear elastic finite element models of the coupled buildings. A set of 10000 ground motion records compatible with the input PSD is generated by using the spectral representation method [45]. This number of samples ensures accurate estimates of the MAF of system failure, ν_f (which is approximately equal to 0.002 for P_{f,t_L} = 10% and t_L = 50 years), with a coefficient of variation approximately equal to 1%.

Fig. 4 compares the system fragility curves obtained analytically and via MCS for the adjacent unconnected buildings (Fig. 4a) and the buildings connected by dampers with c_d = 6000 kN s/m (Fig. 4b). The analytical estimates of $P_{f|IM}(im)$ are computed assuming the two limit conditions of perfect correlation between all pairs of component failures (hereinafter referred to as perfect correlation assumption, which corresponds to the lower bound of the system failure probability) and of statistical independence between any pair of component failures (hereinafter referred to as statistical independence assumption, which corresponds to the upper bound of the system failure probability). Since MCS can accurately account for the statistical dependence among the failure modes, the exact value of the system failure probability according to MCS is also reported in addition to the lower and upper bounds.

The results presented in Fig. 4 indicate that the additional dampers are very effective in reducing the system vulnerability. In particular, the median system capacity evaluated using MCS (i.e., the PGA value corresponding to a 0.5 probability of failure) increases from 0.19 g for c_d = 0 kN s/m to 0.34 g for c_d = 6000 - kN s/m. For the specific problem considered here, the analytical estimates of system fragility $P_{f|IM}(im)$ are usually higher (i.e., more conservative) than the corresponding estimates obtained via MCS, which are considered as the reference solutions. The P approximation is always conservative, while the mVM approximation is the most accurate analytical solution among those considered in this study. The accuracy of the analytical estimates is highest for the case corresponding to c_d = 6000 kN s/m, for which the two systems tend to behave as a single system. This observation is consistent with the results of a previous study of the same authors on a different problem involving the stochastic response of MDOF dynamic systems [14], which showed that the analytical failure probability approximations are most accurate when the response is dominated by a single vibration mode [14].

Based on the MCS results, it is also found that the statistical dependence among the component limit states can affect the system failure probability estimate more than the approximation on the hazard function. For example, Fig. 4 shows that the statistical independence assumption, which is commonly made in computing the system reliability (e.g., in [4,6]), significantly overestimates the system risk. By contrast, the perfect correlation assumption is more accurate (although unconservative), especially for high values of c_d. In fact, the correlation between pairs of limit states reflects the correlation between pairs of interstory drift responses. Since the correlation between pairs of interstory drifts of the two buildings increases for increasing c_d (see Fig. 3), the correlation between pairs of different component limit states is higher for c_d = 6000 kN s/m than for c_d = 0 kN s/m. This phenomenon is also observed in Fig. 4, in which the fragility curve evaluated via MCS (which accounts for the actual statistical dependence among the failure modes) is contained and almost equidistant from the two MCS bounds for c_d = 0 kN s/m, whereas it is almost coincident with the lower bound for c_d = 6000 kN s/m.

Fig. 5 reports the result of a parametric study performed to evaluate, for different damper properties, the effects of approximations on the hazard function and failure modes correlation on the failure risk estimates, P_{f,t_L}, for the two adjacent buildings. The

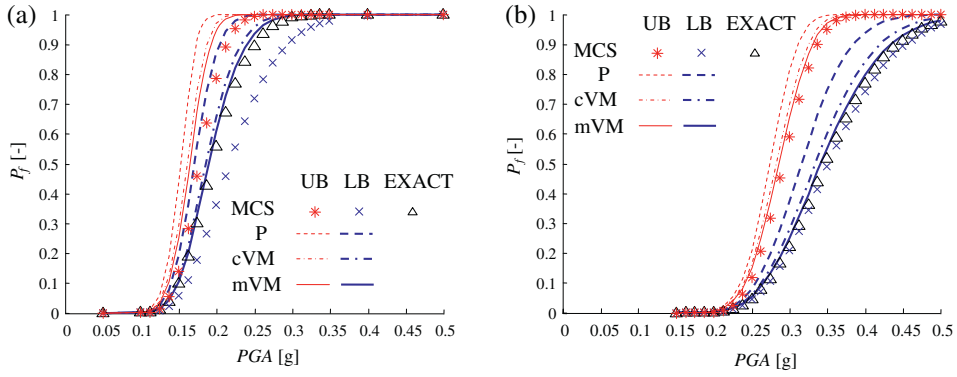

Fig. 4. System fragility curves obtained analytically and via simulation: (a) unconnected adjacent buildings, and (b) buildings connected by dampers with c_d = 6000 kN s/m.

values of the dampers' viscous constant, c_d, vary between 0 and 6000 kN s/m, whereas four different values of dampers' stiffness are considered in the range between $k_d = 0$ kN/m (i.e., purely viscous dampers), and $k_d = 5 \times 10^6$ kN/m (i.e., almost rigid viscoelastic dampers).

It is observed that (1) the use of dampers to connect the adjacent buildings can improve significantly the buildings' performance, and (2) the viscous component of the damper is more effective than the stiffness component in mitigating the seismic risk. In fact, increasing k_d improves the system performance only for very low values of c_d, while in general it results in an increase of the risk. Furthermore, the value of the risk is practically insensitive to the damper stiffness. Similar results are obtained also for other values of k_d (not reported here due to space constraints) and are in agreement with results already available in the literature and based on the analysis of the mean square seismic response of coupled adjacent buildings [3]. The lowest value of P_{f,t_L} is achieved by employing dampers with purely viscous behavior. In the neighborhood of this minimum value, the sensitivity of P_{f,t_L} to changes in the values of c_d is very small. Similar to the results shown in Fig. 4, the results presented in Fig. 5 indicate that the analytical estimates of P_{f,t_L} are more conservative than the estimates obtained through MCS and their accuracy increases for increasing values of c_d. Also in this case, the mVM approximation is the most accurate among the analytical approximations considered in this study. The perfect correlation assumption is more accurate than the statistical independence assumption, especially for high values of c_d and k_d for which the responses of the two adjacent buildings are highly correlated (see Fig. 3b).

4.3. Seismic risk assessment for buildings with uncertain properties and coupled by linear dampers

The effects of MPU on the system reliability of buildings coupled by linear viscous dampers are studied by modeling the dynamic properties of the two buildings as random variables. Following [10], the floor mass and story stiffness of each building are assumed to follow lognormal distributions with mean values equal to the corresponding values considered for the case of deterministic buildings, and with coefficient of variation equal to 0.10 and 0.11, respectively. The damping ratios used to build the Rayleigh damping matrixes for the two buildings are also modeled as random variables with mean value equal to 2% and with coefficient of variation equal to 65% [10]. Since perfect correlation is assumed between the lumped floor masses and between the story stiffness within the same building, the MPU is represented by 6 random variables. Latin hypercube sampling is used to generate 50 samples of structural models [28]. This sample number is sufficient to account with accuracy for the variability of the uncertain parameters, and ensures that the coefficient of variation of the estimates of the failure probability is smaller than 5% for all cases considered. The same sample models are used in correspondence of the different IM values considered in the fragility analysis.

Fig. 6a compares the risk estimates for the buildings with uncertain parameters coupled by linear viscous dampers and varying c_d computed using Latin hypercube sampling in conjunction with the analytical approach and MCS based on 10000 time history analyses. The analytical approximations of the time-variant hazard function provide accurate estimates of the risk, with errors of the same magnitude as those observed for the buildings with deterministic properties. Also in this case, the mVM approximation used in conjunction with the perfect correlation assumption (i.e., the lower bound of the system failure probability) provides the best agreement with MCS results considering the actual statistical dependence among the failure modes.

Fig. 6b compares the risk estimates obtained using MCS for the cases of buildings with deterministic and uncertain properties (in conjunction with Latin hypercube sampling for the case of uncertain buildings). The trend for the seismic risk dependency on c_d is very similar for both the deterministic and uncertain cases. As expected, the seismic risk estimates obtained by considering MPU (denoted as P_{f,t_L}^{UNC}) are always higher than the corresponding estimates obtained by neglecting MPU (denoted as P_{f,t_L}^{DET}). The MPU increases the seismic risk by as much as 25% for low values

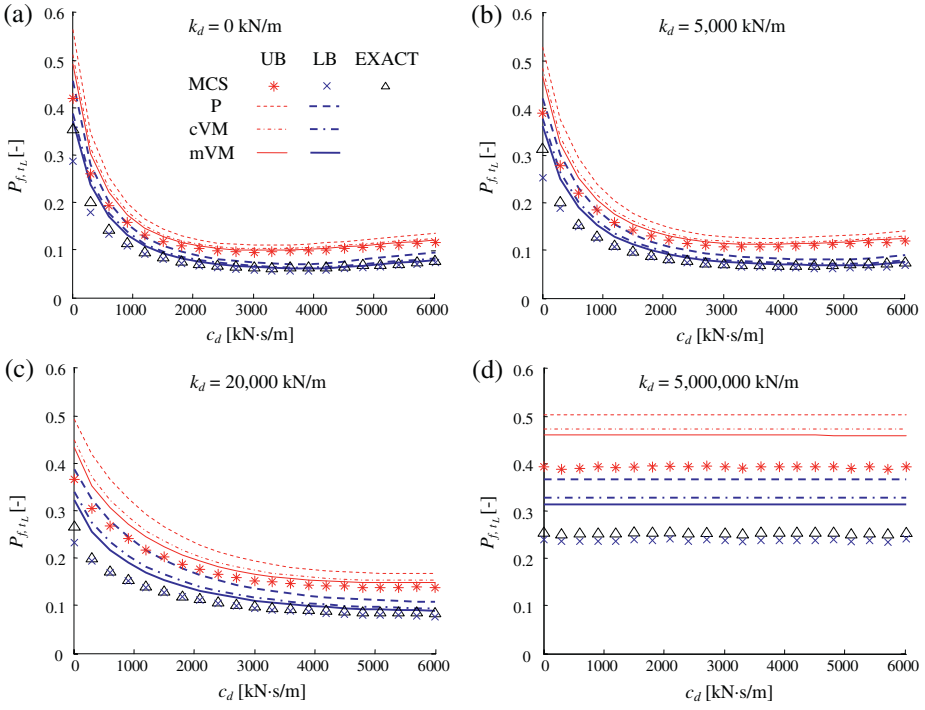

Fig. 5. Probability of exceeding the IO performance level in 50 years for adjacent buildings coupled using linear dampers: (a) $k_d = 0$ kN/m, (b) $k_d = 5000$ kN/m, (c) $k_d = 20000$ kN/m, and (d) $k_d = 5 \times 10^6$ kN/m.

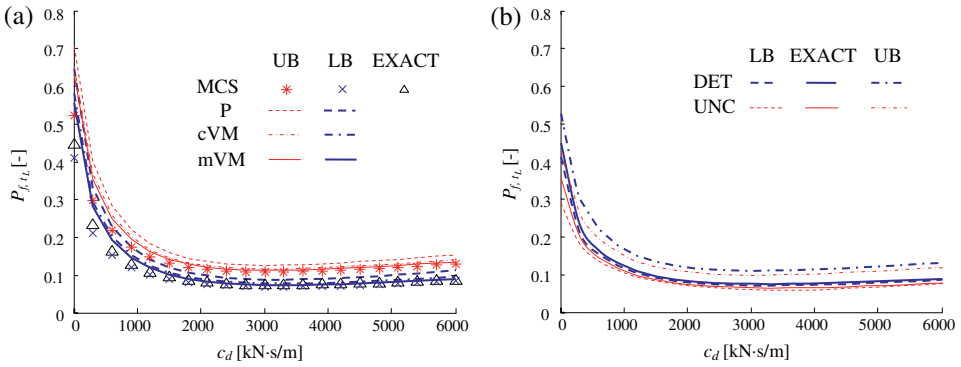

Fig. 6. Effects of MPU on risk estimates: (a) comparison of risk estimates for the buildings with uncertain properties obtained using MCS and the analytical approach, and (b) comparison of risk estimates obtained using the analytical approach for buildings with deterministic and uncertain properties.

of the damping constant when the actual statistical dependence among the failure modes is considered, and as much as 45% when the lower bound (perfect correlation assumption) is considered.

4.4. Seismic risk assessment for buildings with deterministic properties and coupled by nonlinear dampers

This section reports the seismic risk assessment results for the two adjacent buildings with deterministic properties coupled by nonlinear viscous dampers.

Fig. 7 shows the variation with time of the values of the equivalent viscous damping constant, $c_{d,eq}$, corresponding to the dampers that are coupling the adjacent buildings at the four floors, with exponent $\alpha = 0.7$ and viscous constant $c_d = 2500$ kNs$^{0.7}$/m$^{0.7}$, for the two cases of $pga = 0.10$ g (Fig. 7a) and $pga = 0.30$ g (Fig. 7b).

It is observed that the values of the equivalent viscous damping are very high at the beginning and at the end of the seismic excitation (when the seismic excitation is less intense), while they are lower when the seismic excitation is most intense. At a given time instant, the $c_{d,eq}$ values are lower for increasing floor number (i.e., for increasing height). Furthermore, the equivalent damping decreases for increasing seismic intensities. These trends can be explained based on Eq. (10) by observing that (1) the equivalent viscous damping decreases for increasing relative velocities between the dampers' ends, and (2) these relative velocities increase for increasing seismic intensities and floor number.

Fig. 8a compares the analytical and MCS estimates of the risk of exceeding the IO performance level for the adjacent buildings previously described and coupled at the first four floors by nonlinear viscous dampers with equal properties, for a damper exponent $\alpha = 0.7$ and for different values of the damping coefficient c_d. The MCS risk estimates are obtained by employing 100 ground motion records compatible with the input model illustrated in Fig. 2. The analytical estimates are close to the MCS estimates. The discrepancies between the analytical and MCS risk estimates are similar to those observed for the case of buildings coupled by linear viscous dampers and are mainly due to two effects: (1) the stochastic linearization approach, which usually leads to an underestimation of the failure probability [20]; and the use of the P approximation for the time-variant hazard function, which usually results in a overestimation of the failure probability [22]. Also in this case, the analytical risk estimates corresponding to the lower bound assumption for the system reliability provide an approximation that is often sufficiently accurate for engineering approximations, with the exception of buildings coupled with dampers having a very low value of the damper viscous constant, for which the analytical approximations significantly overestimate the MCS results. It is noteworthy that the computational cost of the analytical technique is significantly lower than that of MCS (in this specific case, the analytical technique requires less than 1% of the time required by MCS).

In Fig. 8a, it is also observed that the variation of the system risk with c_d follows a trend similar to that observed for the case of buildings coupled by linear viscous dampers. The value of c_d that minimizes the risk is lower for the case corresponding to $\alpha = 0.7$ than for the linear case (i.e., $\alpha = 1.0$). However, the minimum value of the risk attained with the nonlinear viscous damper is very similar to the corresponding value obtained with the linear dampers (see Fig. 5). In Fig. 8b, the analytical risk estimates obtained for different values of α are plotted as a function of c_d. It is observed that

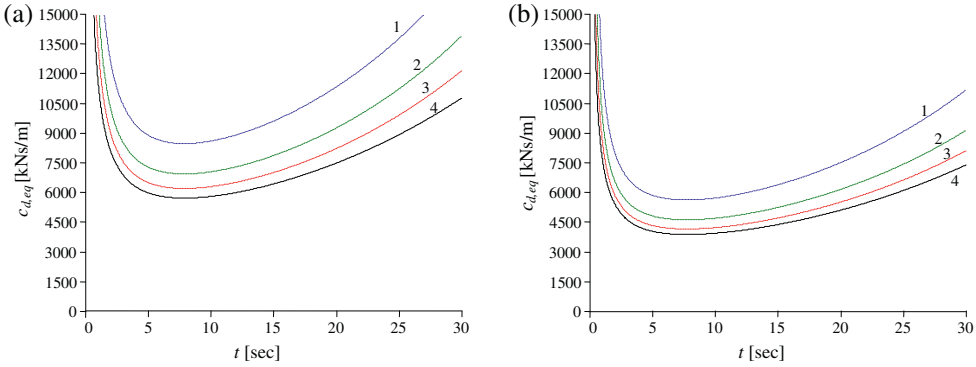

Fig. 7. Time history of the equivalent viscous damping constant, $c_{d,eq}$, of the dampers at the four floors (exponent $\alpha = 0.7$ and viscous constant $c_d = 2500$ kNs$^{0.7}$/m$^{0.7}$): (a) $pga = 0.10$ g, and (b) $pga = 0.30$ g.

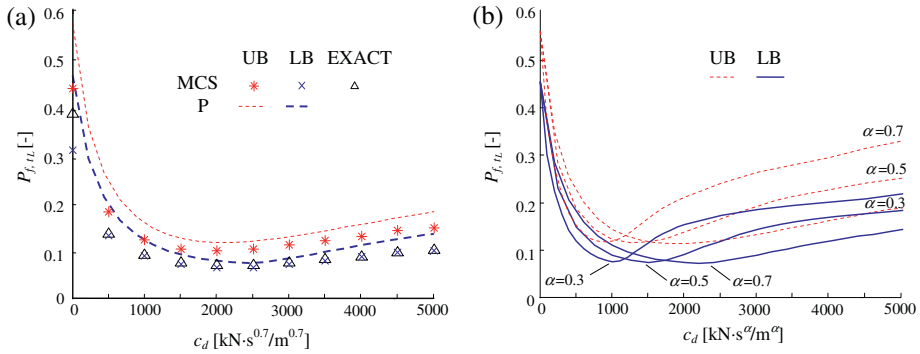

Fig. 8. Probability of exceeding the IO performance level in 50 years for adjacent buildings coupled using viscous dampers as a function of damper viscous constant c_d: (a) comparison of analytical and MCS estimates for $\alpha = 0.7$, and (b) comparison of analytical estimates for different α values.

the value of c_d that minimizes the risk decreases for decreasing values of α, and that dampers with different exponents α provide comparable performances in terms of maximum risk reduction.

5. Conclusions

This study presents a performance-based methodology for the seismic assessment of buildings structures equipped with viscous/visco-elastic damping devices. The proposed methodology, which is consistent with modern performance-based earthquake engineering frameworks, aims at computing the probability of exceeding a target damage level during the design life time of the system, while considering the uncertainty affecting both the seismic input (i.e., record-to-record variability and uncertain intensity level) and the model parameters. The methodology efficiently employs Latin hypercube sampling to account for the uncertainty in the model parameters, Poisson and Vanmarcke approximations to estimate the time-variant failure probability, and recently derived analytical techniques to evaluate the stochastic description (variances, correlation coefficients, and non-geometric spectral characteristics) of the structural response of the buildings.

The capabilities of the proposed methodology are illustrated by analyzing two steel shear-type buildings coupled by viscous/visco-elastic dampers with uniform properties along the height. In the case of linear dampers, a parametric study performed considering both deterministic and uncertain structures for different values of damping constant, c_d, and stiffness constant, k_d, lead to the following observations: (1) the seismic performance of the system is more sensitive to the viscous properties than to the stiffness properties of the dampers; (2) significant variations of c_d result in small variations of the system seismic risk for a wide range of c_d values; (3) the correlation among the various failure modes plays a significant role in the assessment of the system failure probability; (4) the commonly adopted assumption of independent component limit states can result in a significant overestimation of the system seismic risk, in particular for buildings coupled by dampers with high c_d and k_d values; (5) the accuracy of the analytical approximations of the failure probability depends on the system dynamic properties; (6) in most of the cases considered, the estimates obtained by employing the modified Vanmarcke's approximation for the hazard function and by assuming perfect correlation between all pairs of failure modes are sufficiently accurate for engineering purposes; and (7) the effects of model parameter uncertainty on the seismic risk estimate can be significant and should be included in the risk assessment.

The proposed methodology is also applied to the case of nonlinear viscous dampers connecting the adjacent buildings with deterministic properties, and the following conclusions are drawn: (1) the analytical stochastic linearization technique, combined with the methodology proposed in this study, yields risk estimates with an accuracy similar to that achieved in the case of buildings coupled with linear viscous dampers; (2) the value of the nonlinear dampers' viscous constant that minimizes the risk decreases for decreasing values of the velocity exponent; and (3) the use of nonlinear viscous dampers permits to achieve seismic risk reductions similar to those achieved by employing linear viscous dampers.

It is noted here that these conclusions hold only for the specific systems analyzed in this paper. Further studies are required to investigate the accuracy of analytical techniques, stochastic linearization approaches, and time-variant hazard function approximations when they are combined for the evaluation of the seismic reliability of structural systems.

Acknowledgements

The authors gratefully acknowledge support of this research by (1) the Louisiana Board of Regents (LA BoR) through the Pilot Funding for New Research (Pfund) Program of the National Science Foundation (NSF) Experimental Program to Stimulate Competitive Research (EPSCoR) under Award No. LEQSF(2011)-PFUND-225; and (2) the LA BoR through the Louisiana Board of Regents Research and Development Program, Research Competitiveness (RCS) subprogram, under Award No. LESQSF(2010-13)-RD-A-01. Any opinions, findings, conclusions or recommendations expressed in this publication are those of the authors and do not necessarily reflect the views of the sponsors.

References

[1] Soong TT, Spencer BF. Supplemental energy dissipation: state-of-the-art and state-of-the-practice. Eng Struct 2002;24(3):243–59.
[2] Takewaki I. Building control with passive dampers: optimal performance-based design for earthquakes. Singapore: John Wiley & Sons (Asia); 2009.
[3] Xu YL, He Q, Ko JM. Dynamic response of damper-connected adjacent buildings under earthquake excitation. Eng Struct 1999;21(2):135–48.
[4] Guo AX, Xu YL, Wu B. Seismic reliability analysis of hysteretic structure with viscoelastic dampers. Eng Struct 2002;24(3):373–83.
[5] Park KS, Koh HM, Hahm D. Integrated optimum design of viscoelastically damped structural systems. Eng Struct 2004;26(5):581–91.
[6] Marano C, Trentadue F, Greco R. Stochastic Optimum design criterion for linear damper devices for seismic protection of buildings. Struct Multidiscip Optim 2007;33(6):441–55.
[7] Ragni L, Dezi L, Dall'Asta A, Leoni G. HDR devices for the seismic protection of frame structures: experimental results and numerical simulations. Earth Eng Struct Dyn 2009;38(10):1199–217.
[8] Cimellaro GP, Lopez-Garcia D. Algorithm for design of controlled motion of adjacent structures. Struct Control Health Monit 2009;18(2):140–8.
[9] Taflanidis AA, Scruggs JT. Performance measures and optimal design of linear structural systems under stochastic stationary excitation. Struct Saf 2010;32(5):305–15.
[10] Sues RH, Wen YK, Ang AH-S. Stochastic evaluation of seismic structural performance. ASCE J Struct Eng 1985;111(6):1204–18.

[11] Chaudhuri A, Chakraborty S. Reliability of linear structures with parameter uncertainty under nonstationary earthquake. Struct Saf 2006;8(3):231–46.
[12] Dolsek M. Incremental dynamic analysis with consideration of modeling uncertainties. Earth Eng Struct Dyn 2009;38(6):805–25.
[13] Tubaldi E, Barbato M, Dall'Asta A. Influence of model parameter uncertainty on seismic transverse response and vulnerability of steel-concrete composite bridges with dual load path. ASCE J Struct Eng 2012;138(3):363–74.
[14] Tubaldi E, Barbato M, Ghazizadeh S. A probabilistic performance-based risk assessment approach for seismic pounding with efficient application to linear systems. Struct Saf 2012;36–37:14–22.
[15] Beck AT, Gomes WJS. A comparison of deterministic, reliability-based and risk-based structural optimization under uncertainty. Prob Eng Mech 2012;28(3):18–29.
[16] Au S-K, Beck JL. Subset Simulation and its application to seismic risk based on dynamic analysis. J Eng Mech 2003;129(8):901–17.
[17] Jensen HA, Sepulveda JG. On the reliability-based design of structures including passive energy dissipation systems. Struct Saf 2012;34(1):390–400.
[18] Der Kiureghian A, Fujimura K. Nonlinear stochastic dynamic analysis for performance-based earthquake engineering. Earth Eng Struct Dyn 2009;38(5):719–38.
[19] Spanos PD, Kougioumtzoglou IA. Survival probability determination of nonlinear oscillators subject to evolutionary stochastic excitation. ASME J App Mech 2014;81(5):1–9.
[20] Roberts JB, Spanos PD. Random vibration and statistical linearization. NewYork: Dover Publications; 2003.
[21] Barbato M, Vasta M. Closed-form solutions for the time-variant spectral characteristics of non-stationary random processes. Prob Eng Mech 2010;25(1):9–17.
[22] Barbato M, Conte JP. Structural reliability applications of nonstationary spectral characteristics. J Eng Mech 2011;137(5):371–82.
[23] Ghazizadeh S, Barbato M, Tubaldi E. A new analytical solution of the first-passage reliability problem for linear oscillators. J Eng Mech 2012; 136(2):695–706.
[24] Der Kiureghian A. Non-ergodicity and PEER's framework formula. Earth Eng Struct Dyn 2005;34(13):1643–52.
[25] Mackie K, Stojadinovic B. Fragility curves for reinforced concrete highway overpass bridges. In: 13th World Conference on Earthquake Engineering, Vancouver, BC, 2004.
[26] Rüdinger F, Krenk S. Spectral density of an oscillator with power law damping excited by white noise. J Sound Vibr 2003;261(2):365–71.
[27] Di Paola M, Navarra G. Stochastic seismic analysis of MDOF structures with nonlinear viscous dampers. Struct Control Health Monit 2009;16(3):303–18.
[28] McKay MD, Conover WJ, Beckman RJ. A comparison of three methods for selecting values of input variables in the analysis of output from a computer code. Technometrics 1979;21:239–45.
[29] Zhang RH, Soong TT. Seismic design of viscoelastic dampers for structural applications. ASCE J Struct Eng 1992;118(5):1375–92.
[30] Levy R, Lavan O. Closure to "quantitative comparison of optimization approaches for the design of supplemental damping in earthquake engineering practice". ASCE J Struct Eng 2010;136(9):1182–4.
[31] Federal Emergency Management Agency (FEMA), NEHRP guidelines for the seismic rehabilitation of buildings. Washington DC: FEMA Publication 273; 1997.
[32] Federal Emergency Management Agency (FEMA), Prestandard and commentary for the seismic rehabilitation of buildings. Washington DC: FEMA Publication 356; 2000.
[33] Cimellaro GP. Simultaneous stiffness-damping optimization of structures with respect to acceleration, displacement and base shear. Eng Struct 2007;29(11):2853–70.
[34] Freddi F, Tubaldi E, Ragni L, Dall'Asta A. Probabilistic performance assessment of low-ductility RC frames retrofitted with dissipative braces. Earth Eng Struct Dyn 2012;42(7):993–1011.
[35] Dall'Asta A, Ragni L. Dynamic systems with high damping rubber: non-linear behaviour and linear approximation. Earth Eng Struct Dyn 2008; 37(13):1511–26.
[36] Miyamoto HK, Gilani ASJ, Wada A, Ariyaratana C. Limit states and failure mechanisms of viscous dampers and the implications for large earthquakes. Earth Eng Struct Dyn 2010;39(11):1279–97.
[37] Ditlevsen O, Madsen HO. Structural reliability methods. West Sussex: John Wiley & Sons Ltd; 1996.
[38] Pinto PE, Giannini R, Franchin P. Seismic reliability analysis of structures. Pavia: IUSS Press; 2004.
[39] Luco N, Cornell CA. Structure-specific scalar intensity measures for near-source and ordinary earthquake ground motions. Earth Spect 2007; 23(2):357–92.
[40] Lutes LD, Sarkani S. Stochastic analysis of structural and mechanical vibration. New Jersey: Prentice Hall, Upple Saddle River; 1997.
[41] Stefanou G. The stochastic finite element method: Past, present and future. Comput Methods Appl Mech Engrg 2009;198:1031–51.
[42] Barbato M, Tubaldi E. A probabilistic performance-based approach for mitigating the seismic pounding risk between adjacent buildings. Earth Eng Struct Dyn 2013;42(8):1203–19.
[43] Shinozuka M, Sato Y. Simulation of nonstationary random processes. ASCE J Eng Mech Div 1967;93(EM1):11–40.
[44] Clough RW, Penzien J. Dynamics of structures. New York: McGraw-Hill; 1993.
[45] Shinozuka M, Deodatis G. Simulation of stochastic processes by spectral representation. Appl Mech Rev 1991;44(4):191–203.